Ultrasonics 96 (2019) 90–95

Contents lists available at ScienceDirect

Ultrasonics

journal homepage: www.elsevier.com/locate/ultras

A novel ring-beam piezoelectric actuator for small-size and high-precision manipulator

Zilong Ye[a], Chunhua Zhou[b], Jiamei Jin[a,*], Pengpeng Yu[a], Fangyi Wang[a]

[a] State Key Laboratory of Mechanics and Control of Mechanical Structures, Nanjing University of Aeronautics and Astronautics, Nanjing 210016, China
[b] Shanghai Institute of Satellite Engineering, China Aerospace Science and Technology Corporation, Shanghai 200240, China

ARTICLE INFO

Keywords:
Piezoelectric actuator
Joint mechanism
Manipulator

ABSTRACT

A new type of ring (joint)-beam (arm) element based on piezoelectric actuator is designed in this paper. By using piezoelectric ceramics, the vibration modes of two parallel beams are excited and coupled to form in-plane waves on the ring. As the piezoelectric actuator has the dual effect of acting as the power source and the main body structure of the arm joint, compared with the rotating joint using DC motor as the power source, the actuator does not need additional space to install the motor, which makes joint mechanism have the advantages of simple structure and small volume. Furthermore, the micro-displacement control of joints can be achieved by the characteristics of fast response and power self-locking based on the friction driving principle. A two-degree-of-freedom three-arm prototype of the joint mechanism is designed to obtain the parameters of the piezoelectric actuator and carry out related experiments. The prototype of the mechanism is 72 g in weight and 105 mm in length, and the maximum rotation angle of each joint is 210 deg. The experimental results indicate that, when driving frequency is 58.6 kHz and the driving voltage is 300 Vpp, the angular speed of the prototype reaches 45.9 deg/s, the resolution is 0.015 deg and the startup and shutdown response time are 35 ms and 21 ms, respectively. Due to its simple and compact structure, the manipulator have strong growth potential for meeting the requirements of wet hyperbaric environment. The characteristics of fast response time and high resolution enable good mobility and high precision.

1. Introduction

At present, with the gradual improvement of volume, weight and accuracy requirements of detection equipment such as underwater vehicle, its equipped manipulator is also promoted to be lightweight and high-precision [1–3]. The creation of these manipulator provides great convenience for deep-sea exploration and facilitates the assistance of remote control, such as sample collection and equipment maintenance [4–6]. Similarly, a number of unusual joint mechanisms have emerged. Among them, the rapidly developing hydraulic joint mechanism is excellent in large and medium-sized robots (Titan series manipulator joints, Schilling Robotics System, USA, 2012) [7], making the hydraulic servo and remote control manipulator continuously break through the underwater field, but due to its excessive volume and weight, it still has far to make efforts towards lightweight. In addition, the electric manipulator also plays an important role, including the joint mechanisms (Three-Fingered Gripper, Italy, 2013, etc.) [8,9], which can only adapt to the underwater environment with less pressure when operating normally. As a result of it, the miniaturization and high precision joint mechanism adapted to high water pressure need further research.

In view of the joint mechanism of the manipulator, some previous research has been done. Through development, it has the general characteristics of high accuracy, fast time response and power self-locking [10–12]. For instance, in order to drive the joints, the research group proposed an in-plane traveling wave rotary ultrasonic motor (P.R.C, 2008) [13], whose stator is a ring-beam sandwich piezoelectric transducer [14,15]. Its rectangular beam attached to a ring clamp two groups of piezoelectric ceramic piece by bolt. The spring, through the nut on the pressure within the circle of the two conical rotor structure, along the ring axial preload force between stator and rotor. When exciting a traveling wave on the stator ring, the rotor will be rotating by the friction. The structure is simple, compact and easy to miniaturize. Because the low-velocity output does not need decelerating mechanism, and automatic locking does not need locking device. Compared with hydraulic and DC motors, the motor structure is simple, compact and non-lubricated, which can be suitable for underwater work. However, after intensive study, it is found that this kind of mechanism cannot extend its freedom, and it still needs to be improved in space and

* Corresponding author.
E-mail address: jjm@nuaa.edu.cn (J. Jin).

https://doi.org/10.1016/j.ultras.2019.02.007
Received 5 October 2018; Accepted 20 February 2019
Available online 21 February 2019
0041-624X/

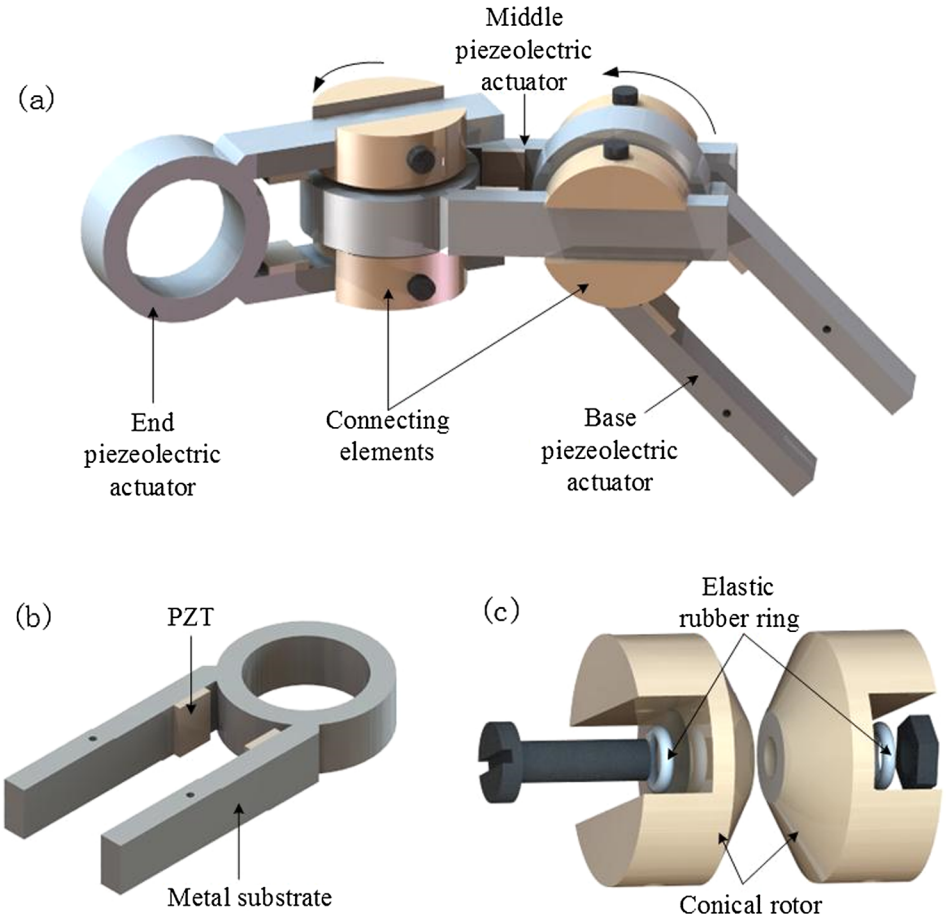

Fig. 1. Configuration view of the mechanism and details. (a) Configuration of the finger. (b) Structure of one piezoelectric actuator. (c) Configuration of joints.

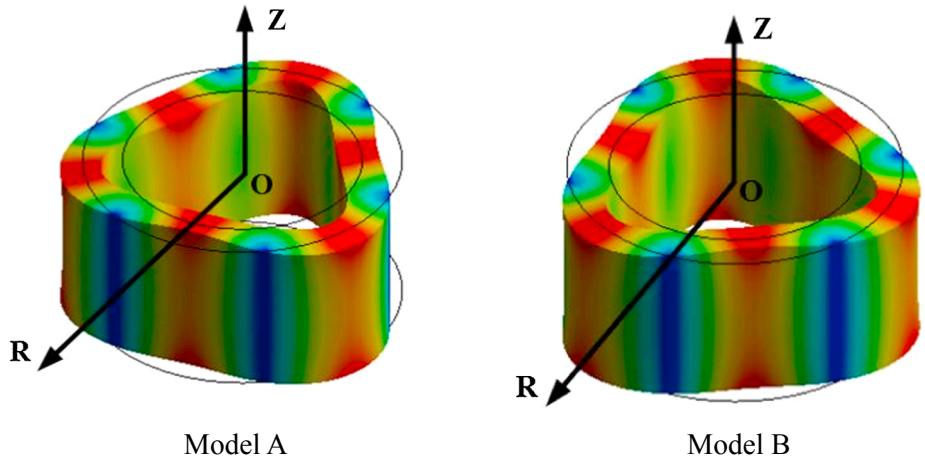

Fig. 2. The orthogonal in-plane bending mode of the ring with the same frequency and mode of vibration.

modularization.

On the whole, the volume of electromagnetic and hydraulic driving manipulator is difficult to control and the weight is large, and it is hard to guarantee long-term sealing, pressure compensation and reduce pollutant emissions in the deep-sea environment. The insulating enveloping manipulator is equipped with various transmission and protective devices, which leads to a significant reduction in accuracy and is not conducive to the realization of remote wireless control.

In order to obtain a small compact joint mechanism, we have developed a type of novel piezoelectric actuator based on the piezoelectric smart materials [16–18] and it can overcome the problems effectively. Features such as the penetration of liquid, the reduction of leakage pollution and high standstill torque what it has are enough for it to be better driver of manipulator. The motion of two degrees of freedom can be realized by orthogonal connection of each joint element, and the concatenation of all joint elements makes structure reach the design requirements of small volume and high degree of freedom. Owing to the lightweight design of material (aluminum alloy) and structure (hollow out), the negative impact on the motion posture of accessories and its manipulator is effectively reduced.

The remainder of this paper is arranged as follows. First of all, the structure and operating principle of the proposed piezoelectric actuator

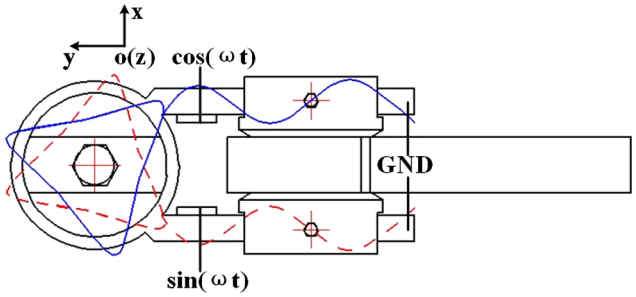

Fig. 3. Operating principle of the piezoelectric actuator.

are presented in Section 2, and then modal analysis of the patched piezoelectric actuator are conducted in Section 3. After that, a two-degree-of-freedom three-arm prototype of the joint mechanism is fabricated and experimented in Section 4. Finally, the conclusion is summarized in Section 5.

2. Configuration and operating principle

2.1. Configuration

The two-degree-of-freedom joint mechanism is composed of three piezoelectric actuators and two joints, which are combined into mechanical structure through orthogonal connection of bolts, as shown in Fig. 1(a). The piezoelectric actuator plays two roles: one as actuators that drive the joint, and the other as bones that form the finger framework. Each piezoelectric actuator includes a metal substrate and two pieces of piezoelectric ceramic (PZT) attached to the metal substrate beam, as shown in Fig. 1(b). The joint consists of two tapered rotor pairs, bolts, nuts, and two elastic ring elements for providing pressure, as shown in Fig. 1(c). The joint mechanism can be used to construct the manipulator with the higher DOF to achieve more functions.

2.2. Operating principle

First of all, in our design, to excite the n_{st} bending vibration modes, piezoelectric actuator is encouraging by its two pieces of piezoelectric ceramic of vibration. The two pieces of PZT patched on beam are excited with a phase difference of $\pi/2$ at the same time. So the vibrating coupled modal can form the in-plane traveling wave on the ring, implementing the rotation of joint. In order to form the B_{0n} in-plane traveling wave of the ring, we need to stimulate two orthogonal B_{0n} in-plane bending vibration modes with the same frequency and mode of vibration. Take the B_{03} mode as an example, as shown in Fig. 2.

Secondly, the joint is driven by contact surface friction, so contact model is particularly important in designing joint mechanisms that require contact friction. In our design, a bending vibration mode generates standing waves on the ring, which makes the inner edge of the ring contact with the conical surface of the joint and drives the joint to rotate through the frictional action.

In terms of signal excitation, the driving ring on the metal substrate is excited by two voltage signals. Overall, it can be seen that the B-phase mode of the driving ring should lead or lag behind the A-phase mode $\pi/2$ phase in time and space to superimpose the rotating traveling wave on the driving ring.

By means of the above two-phase voltage signal excitation, the excitation signals with phase difference of $\pi/2$ in time and space are generated for the two ceramic pieces (the sine-cosine excitation signals are respectively applied to the two beams). The third order bending vibration will be generated by the metal beam, and the spatial $\pi/2$ phase difference between the two third order in-plane bending vibrations formed on the driving ring is shown in Fig. 3. These two modes are coupled on the driving ring to form traveling waves rotating along the circumference, so as to drive the particles on the inner surface of the ring to make micro-amplitude ellipse motion, drive the rotor motion on the inner surface of the ring through friction action, and finally realize the single-degree of freedom motion of the joint. When the two signals phase is difference of $-\pi/2$, the wave of the driving ring will rotate in reverse to realize the reverse drive of the movable joints.

3. Modal analysis

The purpose of modal analysis is to find the optimal geometric parameters of the piezoelectric actuator to produce two third order bending vibration mode. The structure mode is analyzed by the simulation software ANSYS 15.0. The metal matrix material in the mechanism is 6061 aluminum alloy, and the PZT material is 5 * 7 * 1 mm pzt-8 (Seahawks, Suzhou, China). All material parameters are listed in Table 1, after optimization through modal analysis, the geometric parameters are listed in Table 2. The specific meaning of the parameters is illustrated in Fig. 4. The frequency of two third order bending modes of piezoelectric actuators is illustrated in Fig. 5. The simulation frequency is 61.529 kHz and 61.566 kHz, respectively. In addition, the interference modes are 51.286 kHz and 63.782 kHz respectively, far away from the required mode frequency.

4. Experiments and analysis

According to the above theoretical analysis, three piezoelectric actuators were processed and assembled into a prototype of the joint mechanism, as shown in Fig. 6. The size of the prototype (105 mm × 21 mm × 21 mm) is about 1.5 times that of the human hand and the weight is 72 g.

4.1. Experiment on vibration characteristics of piezoelectric actuator

In order to find the third order bending mode, the laser scanning vibration measurement system (psv300f-b, Polytec, Inc. Waldbronn, Germany) conduct a vibration characteristic test. The amplitude-frequency curve of piezoelectric actuator is plotted in Fig. 7. The measured modal frequency is 58.453 kHz and 58.938 kHz respectively, indicating that the difference in resonant frequency between the two operating

Table 1
Material parameters of piezoelectric actuator.

Materials	Young's modulus (GPa)	Piezoelectric constant (C/m^2)	Poisson's ratio	Density (kg/m^3)
Phosphor bronze	113	/	0.33	8800
PZT-8	$\begin{bmatrix} 12.06 & 5.35 & 5.15 & 0 & 0 & 0 \\ 0 & 12.06 & 5.15 & 0 & 0 & 0 \\ 0 & 0 & 10.45 & 0 & 0 & 0 \\ 0 & 0 & 0 & 3.13 & 0 & 0 \\ 0 & 0 & 0 & 0 & 3.13 & 0 \\ 0 & 0 & 0 & 0 & 0 & 3.46 \end{bmatrix}$	$\begin{bmatrix} 0 & 0 & -5.2 \\ 0 & 0 & -5.2 \\ 0 & 0 & -5.2 \\ 0 & 0 & 0 \\ 0 & 12.7 & 0 \\ 12.7 & 0 & 0 \end{bmatrix}$	/	7600

Table 2
Geometric parameters of piezoelectric actuator.

Parameters	L1	L2	L3	L4	L5	D1	D2	θ1
Value	12 mm	3.25 mm	40 mm	7 mm	1.5 mm	15 mm	21 mm	90 deg

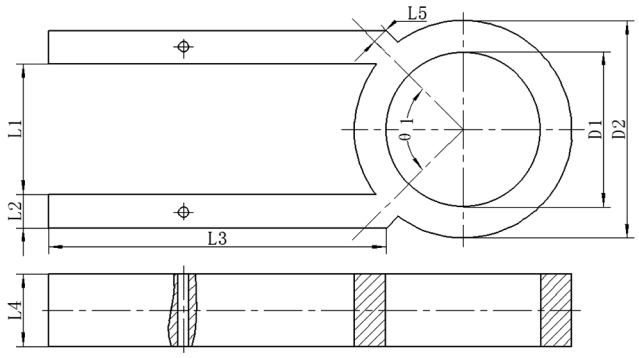

Fig. 4. Geometric parameters of the piezoelectric actuator.

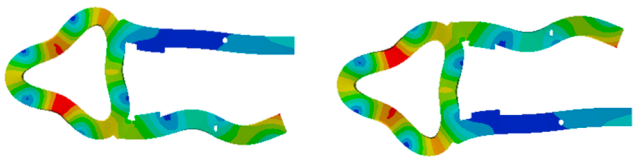

Fig. 5. Third order bending vibration mode calculated by modal analysis.

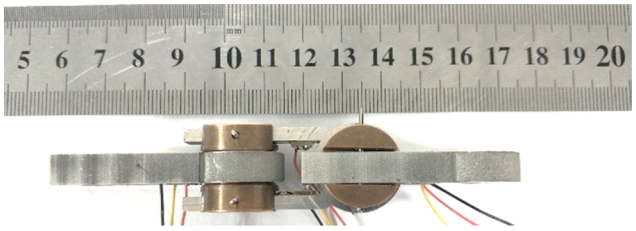

Fig. 6. The prototype of joint mechanism.

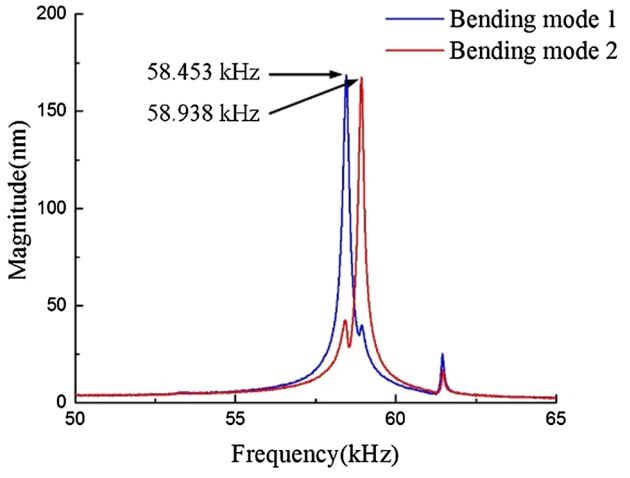

Fig. 7. Vibration characteristic measurement result of two piezoelectric actuators.

vibration modes is 485 Hz, which is slightly different from the modal analysis results. Considering the difference of material and assembling error, the discrepancy is acceptable.

4.2. Frequency sensitivity of joint mechanism

A laser displacement sensor (LK-H050, Keyence Corp, Osaka, Japan) was used to investigate the frequency sensitivity of the piezoelectric actuator in order to measure the operating frequency range of the joint mechanism. The base piezoelectric actuator is fixed on the experimental setup, which is shown in Fig. 8. When the middle piezoelectric actuator is measured, two excitation voltages with 300 Vpp with a phase difference of π/2 are applied on base actuator simultaneously. So as to measurement of the end piezoelectric actuator, the excitation voltages are applied on the middle actuator. The average velocity-frequency results between the middle and the end actuator are shown in Fig. 9. The variation trend of them is as follows: at the beginning, the average velocity increases with the increase of frequency. When the frequency is between 58.5 kHz and 58.8 kHz, the average velocity tends to the maximum, up to 45.9 deg/s, and then decreases with the increase of frequency. The difference of their velocities is caused by the assembling error and different boundary condition.

4.3. Measurement of angular velocity of joint mechanism

The average velocity is not only related to frequency, but also closely related to driving voltage. Therefore, we establish the relation between the average velocity and driving voltage. According to the frequency response testing results, 58.6 kHz is selected as the driving frequency. The experimental results show that the both speeds of increase with the increase of driving voltage is proportional to driving voltage, as shown in Fig. 10. The rotational velocities in two vertical directions of the actuators have the same trend as voltage increases, and the values are very close to each other, as also shown in Fig. 10. Considering the fact that the preload between two conical rotors is forced by bolt and nut which lead to the different contact situation, the velocity difference is acceptable.

4.4. Micro-displacement response of the joint mechanism

The micro-displacement response of the joint mechanism is an important index to realize accurate operation of the actuator. The micro-displacement response is obtained by measuring the step-period and transient characteristics of the actuator. The measurement results show that, driven by a voltage of 300 Vpp and frequency of 58.6 kHz, the resolution can reach up to 15 m deg, as shown in Fig. 11. The startup and shutdown response time under the same conditions are 35 ms and 21 ms, as shown in Fig. 12. The micro-displacement response of the joint mechanism makes it have great potential in the complex working environment.

5. Conclusion

In this paper, we have successfully designed and manufactured a novel piezoelectric driven joint mechanism. The joint mechanism consists of three piezoelectric actuators comprising two joint parts. Through the inverse piezoelectric effect of the piezoelectric ceramic piece, the third order bending vibration mode of two parallel beams is excited and coupled to form in-plane traveling waves on the ring. The prototype of joint mechanism is assembled and shaped according to the design requirements after simulation and structure optimization. The switchboard weighs 72 g and is 105 mm long, with a maximum rotation angle of 210 deg. The experimental results show that when the drive

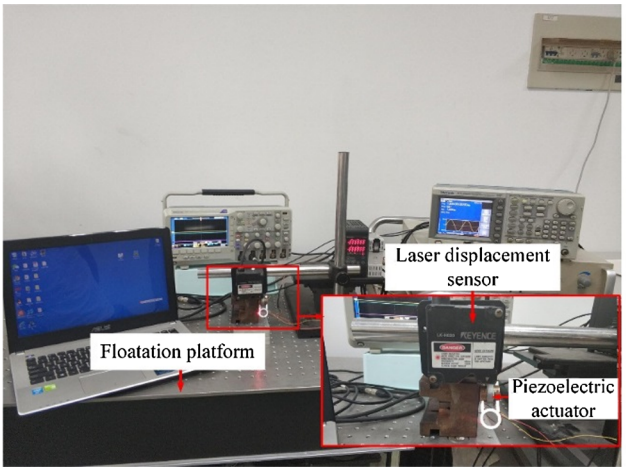

Fig. 8. Experiment setup for joint mechanism.

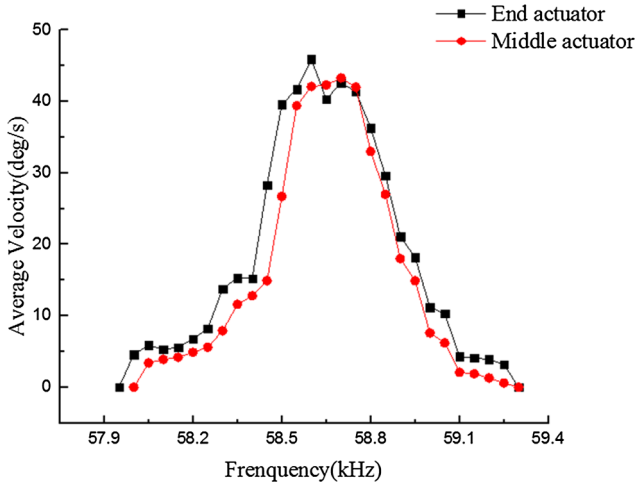

Fig. 9. Frequency sensitivity experimental results.

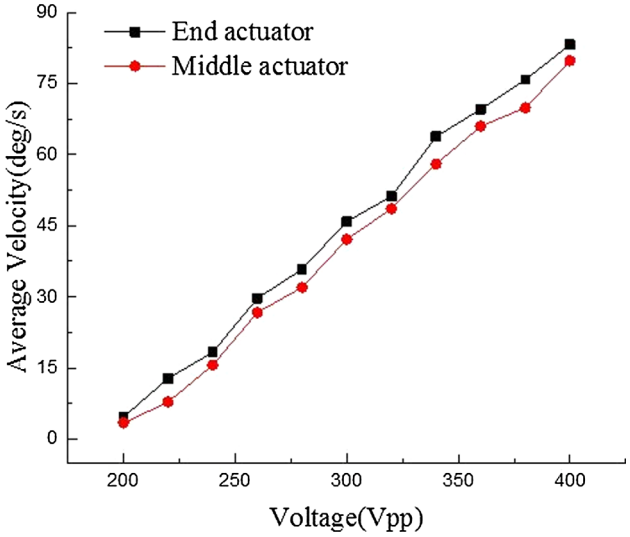

Fig. 10. Relation between average velocity and driving voltage.

frequency is 58.6 kHz and the drive voltage is 300 Vpp, the average speed of the prototype is 45.9 deg/s. Its rotational sensitivity is 0.015 deg, and its startup and shutdown response time are 35 ms and 21 ms. The ring-beam piezoelectric actuator has great potential to adapt

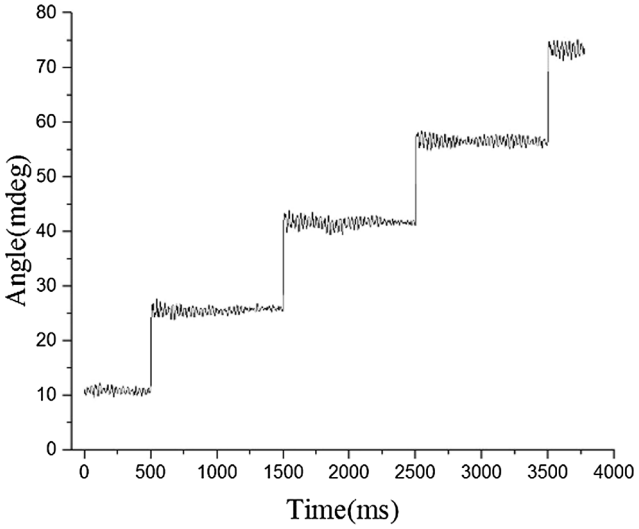

Fig. 11. Resolution of the end actuator under driving voltage of 300 Vpp at 58.6 kHz.

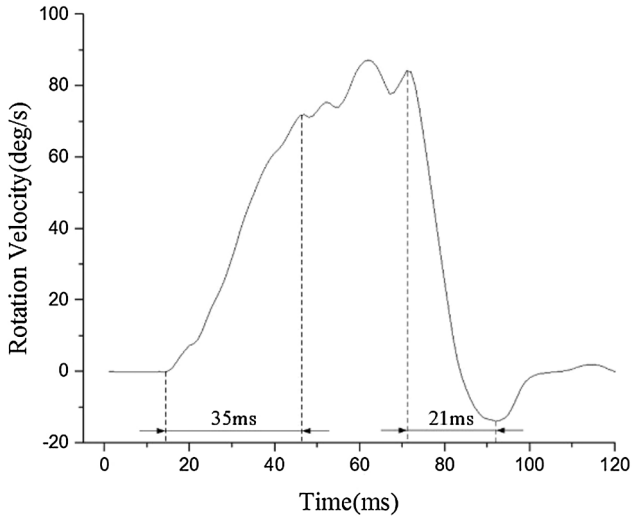

Fig. 12. Transient response of the end actuator under driving voltage of 300 Vpp at 58.6 kHz.

to the complex working environment, and the characteristics of fast response time and high resolution enable good mobility and high precision. According to the above finding, the piezoelectric actuator has the ability to operate on the underwater environment and has the great hopeful to be applied to the work of autonomous underwater vehicles (AUV).

Acknowledgements

This research was supported by the National Natural Nature Science Foundation of China (Grants Nos. 51775263), the funding of Laboratory Open Fund in NUAA (Grants No. KFJJ20180103), and a Project Funded by the Priority Academic Program Development of Jiangsu Higher Education Institutions (PAPD).

Appendix A. Supplementary material

Supplementary data to this article can be found online at https://doi.org/10.1016/j.ultras.2019.02.007.

References

[1] Shigeo Hirose, Yoji Umetani, The development of soft gripper for the versatile robot hand, Mech. Machine Theory 13 (3) (1978) 351–359.
[2] N. Harris, M. Hill, Y. Shen, et al., A dual frequency, ultrasonic, microengineered particle manipulator, Ultrasonics 42 (1) (2004) 139–144.
[3] S. Sivčev, M. Rossi, J. Coleman, et al., Collision detection for underwater ROV manipulator systems, Sensors (2018) 18(4).
[4] P. Boltryk, M. Hill, A. Keary, et al., An ultrasonic transducer array for velocity measurement in underwater vehicles, Ultrasonics 42 (1) (2004) 473–478.
[5] K. Kilteni, J.M. Normand, M.V. Sanchez-Vives, et al., Extending body space in immersive virtual reality: a very long arm illusion, Plos One 7 (7) (2012).
[6] B. Yao, F. Bu, J. Reedy, et al., Adaptive robust motion control of single-rod hydraulic actuators: theory and experiments, IEEE/ASME Trans. Mechatron. 5 (1) (2002) 79–91.
[7] S.C. Robinson, R.E. Pollard, E.W. Walker, et al., Schilling Titan 7 plasma spray system, 1994.
[8] J.R. Bemfica, C. Melchiorri, L. Moriello, et al., A three-fingered cable-driven gripper for underwater applications, IEEE International Conference on Robotics and Automation, IEEE, 2014, pp. 2469–2474.
[9] Q. Zhang, Y. Zhang, L. Huo, et al., Design and pressure experiments of a deep-sea hydraulic manipulator system 8917(2) (2014) 117–128.
[10] R. Ji, J. Jin, L. Wang, et al., A novel ultrasonic surface machining tool utilizing elastic traveling waves, Ultrasonics 80 (2017) 78–86.
[11] W. Zhang, H. Xu, X. Ding, Design and dynamic analysis of an underwater manipulator, Proceedings of the 2015 Chinese Intelligent Automation Conference, Springer, Berlin, Heidelberg, 2015, pp. 399–409.
[12] S. Mcmillan, D.E. Orin, R.B. Mcghee, Efficient dynamic simulation of an unmanned underwater vehicle with a manipulator, IEEE International Conference on Robotics and Automation, 1994. Proceedings, vol.2, IEEE, 1995, pp. 1133–1140.
[13] L. Paull, S. Saeedi, M. Seto, et al., AUV navigation and localization: a review, IEEE J. Oceanic Eng. 39 (1) (2014) 131–149.
[14] V.M. Hernández-Guzmán, R. Campa, PID control of robot manipulators equipped with brushless DC motors, Robotica 27 (2) (2009) 225–233.
[15] Jiang Zheng, Liang Wang, Jiamei Jin, A novel robotic arm driven by sandwich piezoelectric transducers, Ultrasonics 84 (2018) 373–381.
[16] R. Ji, J. Jin, L. Wang, et al., A novel ultrasonic surface machining tool utilizing elastic traveling waves, Ultrasonics 80 (2017) 78–86.
[17] J. Jin, C. Zhao, A novel traveling wave ultrasonic motor using a bar shaped transducer, J. Wuhan Univ. Technol. 23 (6) (2008) 961–963.
[18] H. Kamath, M. Willatzen, R.V. Melnik, Vibration of piezoelectric elements surrounded by fluid media, Ultrasonics 44 (1) (2006) 64–72.